HHS Public Access

Author manuscript

Metab Eng. Author manuscript; available in PMC 2017 September 01.

Published in final edited form as:

Metab Eng. 2016 September ; 37: 24–34. doi:10.1016/j.ymben.2016.04.001.

Extreme promiscuity of a bacterial and a plant diterpene synthase enables combinatorial biosynthesis

Meirong Jia[a], **Kevin C. Potter**[a,†], and **Reuben J. Peters**[a,*]

[a]Roy J. Carver Department of Biochemistry, Biophysics & Molecular Biology, Iowa State University, Ames, IA 50011, USA

Abstract

Diterpenes are widely distributed across many biological kingdoms, where they serve a diverse range of physiological functions, and some have significant industrial utility. Their biosynthesis involves class I diterpene synthases (DTSs), whose activity can be preceded by that of class II diterpene cyclases (DTCs). Here, a modular metabolic engineering system was used to examine the promiscuity of DTSs. Strikingly, both a bacterial and plant DTS were found to exhibit extreme promiscuity, reacting with all available precursors with orthogonal activity, producing an olefin or hydroxyl group, respectively. Such DTS promiscuity enables combinatorial biosynthesis, with remarkably high yields for these unoptimized non-native enzymatic combinations (up to 15 mg/L). Indeed, it was possible to readily characterize the 13 unknown products. Notably, 16 of the observed diterpenes were previously inaccessible, and these results provide biosynthetic routes that are further expected to enable assembly of more extended pathways to produce additionally elaborated ‘non-natural’ diterpenoids.

Keywords

Diterpenes; Diterpene synthases; Metabolic engineering; Substrate specificity

Chemical compounds

Sclareol; *ent*-sclareol; kolavelool; *ent*-kolavelool; vitexifolin A; viteagnusin D; *iso*-abienol; *ent*-manoyl oxide; *ent*-manool; nosyberkol

1. Introduction

Diterpenes are widely distributed metabolites that exhibit various biological functions. For example, the gibberellin plant hormones are essential for normal plant development (Sun, 2011). In addition, many more-specialized diterpenes serve various ecological roles – *e.g*, as

*Corresponding author: address: rjpeters@iastate.edu.

†Current address: Department of Biology, University of North Carolina, Raleigh, NC

phytoalexins produced against infection in cereal crop plants (Schmelz et al., 2014), or allelochemicals in rice (Kato-Noguchi and Peters, 2013). Notably, several diterpenes also are widely used in industry – *e.g.*, sclareol and *cis*-abienol are precursors for synthesis of the perfuming agent ambroxide (Caniard et al., 2012; Schalk et al., 2012), and others are pharmaceutical agents, such as Taxol and the tanshinones (Croteau et al., 2006; Guo et al., in press).

(*E,E,E*)-Geranylgeranyl diphosphate (GGPP, **1**)[1] serves as the general diterpene precursor. However, it has recently been shown that the *cisoid* analog (*Z,Z,Z*)-nerylneryl diphosphate (NNPP, **2**) can serve a precursor as well (Zi et al., 2014b). This result suggests that diterpenes may be more broadly derived from various precursors with a variety of double-bonds configurations and potentially even irregularly (i.e., not just head-to-tail) joined isoprenyl units, as suggested by the production of such compounds by certain isoprenyl diphosphate synthases (Noike et al., 2008; Teufel et al., 2014). Nevertheless, among diterpenes the labdane-related super-family stands out for its sheer size, as these comprise almost 7,000 of the 12,000 known such natural products (Peters, 2010). This super-family is characterized by a core decalin ring structure produced by the initiating class II diterpene cyclases (DTCs), from GGPP – *e.g.* the eponymous labdadienyl/copalyl diphosphate (CPP) (Peters, 2010). These bicyclic diphosphate esters are then typically further transformed by subsequently acting class I diterpene synthases (DTSs) that catalyze lysis/ionization-initiated cationic cyclization and/or rearrangement reactions, leading to a structurally diverse range of diterpenes with varied biological and industrial functions, such as the gibberellin phytohormones and the potential pharmaceutical tanshinones.

Due to the interesting activities associated with diterpene natural products their biosynthesis has been extensively investigated (Zi et al., 2014a). This is perhaps most advanced with regards to diterpene cyclases/synthases, significant numbers of which have been identified over the last two decades. These studies have relied on recombinant expression of these DTCs and/or DTSs in heterologous organisms ranging from bacteria to yeast and tobacco plants, often with co-expression of a GGPP synthase to provide this precursor in a metabolic engineering approach that enables product characterization upon simple extraction, including combining native pairs of labdane-related diterpene cyclases/synthases (Zerbe and Bohlmann, 2015).

Recent results have highlighted the structural diversity that can be generated by DTCs. While these all catalyze bicyclization of GGPP, this can occur in four possible configurations, and can be followed by rearrangement and/or the addition of water prior to concluding deprotonation (Fig. 1). Thus, DTCs can generate three basic types of bicyclic

[1]**Abbreviations:** DTCs, diterpene cyclases; DTSs, diterpene synthases; KgTS, terpentetriene synthase from *Kitasatospora griseola;* SsSS, sclareol synthase from *Salvia sclarea*; GGPP, (*E,E,E*)-geranylgeranyl diphosphate; NNPP, (*Z,Z,Z*)-nerylneryl diphosphate; GGPS, (*E,E,E*)-geranylgeranyl diphosphate synthase; CPP, copalyl diphosphate; Rv3378c, tuberculosinol synthase from *Mycobacterium tuberculosis;* NNPS, (*Z,Z,Z*)-nerylneryl diphosphate synthase; AgAS, abietaenol synthase from *Abies grandis*; SmCPS/KSL1, labda-7,13*E*-dien-15-ol synthase from *Selaginella moellendorffii*; NgCLS, 8α-hydroxy-CPP synthase from *Nicotiana glutinosa;* MvCPS1, peregrinol diphosphate synthase from *Marrubium vulgare;* An2, *ent*-CPP synthase from *Zea mays;* AtCPS, *ent*-CPP synthase from *Arabidopsis thaliana*; OsCPS4, *syn*-CPP synthase from *Oryza sativa;* Haur_2145, kolavenyl diphosphate synthase from *Herpetosiphon aurantiacus;* KgTPS, terpentedienyl diphosphate synthase from *Kitasatospora griseola;* MtHPS, tuberculosinyl/halimadienyl diphosphate synthase from *Mycobacterium tuberculosis;* IPTG, isopropylthiogalactoside.

scaffolds, corresponding to labdanes, halimadanes and clerodanes (Peters, 2010). Each of these can be generated in differing stereochemistries, resulting from differing conformations of GGPP (Peters, 2010), which can perhaps be most readily observed in the initially formed labdadienyl bicycles by examination of the configuration of carbons 9 and 10 (C9 and C10; see Fig. 1 for numbering). Immediate deprotonation at the C8-methyl yields CPP (labda-8(17),13-dienyl diphosphate), traditionally designated as normal (**3**, with absolute configuration of 9*S*,10*S*), *ent*- (**4**, with 9*R*,10*R*), *syn*- (**5**, with 9*R*,10*S*), or *syn*-*ent*- (with 9*S*, 10*R*, although this has not yet been observed) – note that the configuration of the C5-hydrogen is always *trans* to the C10-methyl in these. While CPP production is quite common, deprotonation can occur at alternative positions, such as C7, generating double bond isomers such as *endo*-CPP (labda-7,13-dienyl diphosphate, **6**) (Mafu et al., 2011). Alternatively, water can be added to the initially formed labda-13*E*-en-8-yl^{+} diphosphate carbocation prior to deprotonation, to yield a hydroxylated product (*e.g.* labda-13*E*-en-8α-ol diphosphate, **7**), producing further chemical diversity (Falara et al., 2010). Moreover, the initially formed labda-13*E*-en-8-yl^{+} diphosphate carbocation can undergo rearrangement as well, typically through a series of 1,2-shifts of hydride and methyl groups, although modulation of the initially formed decalin ring structure also has been suggested to occur (Peters, 2010). Each of the resulting carbocationic intermediates can undergo the addition of water prior to deprotonation, which otherwise often can occur at more than one location, giving rise to various double-bond isomers, further increasing the resulting chemical complexity. To date, through cloning from native sources and/or enzyme engineering efforts, DTCs catalyzing the production of 12 distinct products are known (see Table 1).

However, the scarcity and specificity of subsequently acting DTSs largely restricts our ability to access the full structural diversity of diterpenes. In particular, most of DTSs characterized thus far exhibit both regio- and stereo-specificity, as exemplified by *ent*-kaurene synthases from rice and lettuce (Shimane et al., 2014), which only showed activity towards *ent*-CPP (**4**), although a few DTSs have been found that react with more than one CPP stereoisomer, as exemplified by several DTSs from cereal crop plants (Morrone et al., 2011; Zhou et al., 2012).

Intriguingly, the terpentetriene synthase from *Kitasatospora griseola* (Dairi et al., 2001; Hamano et al., 2002), termed here KgTS, and the sclareol synthase from *Salvia sclarea* (Caniard et al., 2012; Schalk et al., 2012), termed here SsSS, have both been reported to exhibit some substrate promiscuity (Ignea et al., 2015; Nakano et al., 2010). However, these studies were somewhat limited in the number of potential substrates examined. Here both were investigated with both the two known linear precursors **1** and **2**, and the 12 currently available bicyclic DTC products (**3** – **14**) via a modular metabolic engineering system in a combinatorial biosynthetic approach. Strikingly, both KgTS and SsSS reacted with all 12 bicycles and even one or two linear precursors with reasonable efficiency, as demonstrated by facile production of sufficient amounts for structural characterization of the 13 observed unknown enzymatic products.

2. Results

2.1. Modular metabolic engineering reveals extreme promiscuity

To probe the full extent of the substrate promiscuity of KgTS and SsSS, a previously developed modular metabolic engineering system was utilized. This system enables facile co-expression of DTCs and DTSs in *E. coli* also engineered to produce **1** via co-expression of a GGPP synthase as well (Cyr et al., 2007). Moreover, it is possible to readily further increase flux towards isoprenoid metabolism (Morrone et al., 2010), which allows production of sufficient amounts of the resulting diterpenes for purification and structural analysis by NMR from reasonably small culture volumes (≤ 3 L). The system has further proved amendable to incorporation of an NNPP rather than GGPP synthase for the production of **2** as a diterpene precursor instead of **1** (Zi et al., 2014b).

This system has been employed to determine the stereochemistry of DTC product outcome and probe the substrate specificity of DTSs from both plants and microbes (Cui et al., 2015; Gao et al., 2009; Hershey et al., 2014; Jackson et al., 2014; Lu et al., 2015; Morrone et al., 2009; Wu et al., 2012; Xu et al., 2014), revealing limited promiscuity of DTSs in certain cases (Mafu et al., 2015; Morrone et al., 2011; Zhou et al., 2012). Strikingly, attempts to use SsSS to investigate DTC product stereochemistry, specifically with 8β-hydroxy-*ent*-CPP (**8**) that is enantiomeric to its native substrate, suggested a surprising degree of promiscuity, at least relative to other previously investigated plant DTSs. In particular, SsSS readily reacts with **8** and produces a further hydroxylated product.

To fully explore this intriguing observation, an array of DTCs with varied product outcome, a total of 12 (**3** – **14**; Table 1), was assembled into the metabolic engineering system (Table S1) for co-expression with SsSS. In addition, the difference in product outcome generally mediated by KgTS, simple removal of the diphosphate to yield an additional carbon-carbon double bond, relative to SsSS, which prototypically installs a hydroxyl group via the addition of water to the tertiary position of the allylic carbocation resulting from diphosphate lysis, prompted investigation of this functionally distinct DTS as well. Given the previously reported ability of KgTS to react with **1** in vitro (Nakano et al., 2010), both this and SsSS also were co-expressed with only a GGPP or NNPP synthase (i.e., to determine their ability to react with **1** or **2**, respectively).

While KgTS has previously been shown to react with five DTC products as well as **1** (Nakano et al., 2010), these studies were carried out in vitro, and it was unclear how relevant such activity would be in the context of an in vivo (albeit heterologous) setting. In particular, there are endogenous (*E. coli*) phosphatases that will act upon **1**, **2** and DTC products, yielding the corresponding primary alcohols, which are easily extractable from the bacterial culture and observable by GC-MS analysis (these peaks are designated by prime' notation of the number corresponding to the diphosphate precursor – i.e., **1′** – **14′**). Both SsSS and KgTS outcompete these endogenous phosphatases for **1** (Fig. 2), with KgTS producing the previously reported mixture of three double bond isomers of springene (**15 – 17**), with the major product being the *exo*-methylene containing β-springene (Hamano et al., 2002), while SsSS produces the tertiary alcohol geranyllinalool (**18**), as identified by comparison of retention time and mass spectrum to an authentic standard upon GC-MS analysis (Fig. S1).

By contrast, KgTS does not seem to react with **2**, and SsSS does so rather inefficiently, producing a mixture of unidentified compounds (Fig. S2).

As expected, each of the DTCs utilized here efficiently converted **1** into their particular bicyclic product (Fig. 3). Given that the native substrate for both SsSS and KgTS are DTC products, it seemed unlikely that either would effectively compete with the DTCs for **1**. Consistent with this expectation, in none of the DTC co-expression cultures tested here were the linear SsSS or KgTS products observed (i.e., geranyllinalool or springenes). On the other hand, both SsSS and KgTS reacted quite effectively with all 12 DTC products tested here, at least relative to competition with the endogenous phosphatases. Indeed, in only a few cases are more than trace amounts of the dephosphorylated DTC product observed (for relative conversion percentages see Fig. S3).

2.2 DTC+DTS product identification

The observed mass spectra are consistent with the previously reported activity of SsSS and KgTS with their native substrates – i.e., the production of sclareol (**19**) from **7** by SsSS (Caniard et al., 2012; Schalk et al., 2012), and terpentetriene (**20**) from terpentedienyl diphosphate (**9**) by KgTS (Dairi et al., 2001). Similarly, SsSS reacts with the stereo-equivalent normal CPP (**3**) to produce manool (**21**), as previously reported (Ignea et al., 2015), and KgTS reacts with **3** – **5** and tuberculosinyl diphosphate (**10**), producing the previously reported triene derivatives (Nakano et al., 2010); specifically, sclarene (**22**, from **3**), (*Z*)-biformene (**23**, from **4**), griseolaene (**24**, from **5**), and tuberculosene (**25**, from **10**). The mass spectra for **19** – **25** can be found in the Supporting Information (Fig. S4).

In a number of cases it seemed likely that the observed products matched previously reported DTS products, which was investigated by co-expression of the relevant DTS and comparison of the retention time and mass spectra of the resulting product(s) with those from SsSS or KgTS. In this manner, KgTS was found to produce *cis*-abienol (**26**) as the minor product (~35%) with **7** by comparison to the previously reported product of a bifunctional DTC/DTS from *Abies balsamea* (Zerbe et al., 2012)(Fig. S5), and *ent*-manoyl oxide (**27**) from **8** (Fig. S6), representing the only further cyclized product, by comparison to the previously reported facile production of such heterocycles by a number of DTSs, although this was only a very minor product of those enzymes (Mafu et al., 2015), and so KgTS offers novel biosynthetic access to **27**. By similar comparisons, SsSS was found to produce *ent*-manool (**28**) from **4** (Fig. S7), vitexifolin A (**29**) from **5** (Fig. S8), and isotuberulosinol/nosyberkol (**30**) from **10** (Fig. S9), by comparison to the previously reported products of the enzyme encoded by *Rv3378c* in *Mycobacterium tuberculosis* with these same substrates (Hoshino et al., 2011; Maugel et al., 2010; Nakano et al., 2011). Notably, Rv3378c does not efficiently react with these substrates in the context of this bacterial metabolic engineering system (Figs. S7 – 9), which presumably stems from the recent discovery that it primarily acts as an adenosine prenyl transferase rather than DTS (Layre et al., 2014). Accordingly, the SsSS activity reported here provides a much more efficient biosynthetic route to **28** – **30**.

In a number of cases the observed products could not be identified by comparison to readily available compounds, and it was necessary to obtain sufficient amounts of these for structural analysis by NMR. This was readily accomplished by simply growing larger volumes of the relevant cultures, with over-expression of several key enzymes involved in the endogenous isoprenoid precursor supply pathway to increase flux to terpenoid metabolism (Morrone et al., 2010). Indeed, in one case it was possible to further generate the higher amounts necessary for investigation of chirality by optical rotation. In particular, with the only known DTC that produces *endo*-CPP (**6**) the absolute stereochemistry has not yet been defined (Mafu et al., 2011). Both SsSS and KgTS readily react with **6**, with yields of ~15 mg/L for these non-native un-optimized DTC/DTS combinations. Upon purification of these products, the correlations observed in their respective 2D DQF-COSY, HMQC-COSY HSQC, HMBC spectra established the positions of the newly formed hydroxyl-group in the SsSS product and the carbon-carbon double bond in the KgTS product, while NOESY spectra were used to confirm the relative configuration of chiral carbons (Figs S10 – S13 and Tables S2 & S3). The specific optical rotation value of the KgTS product was then determined to be $[\alpha]_D^{25}$ = +27 (c = 3.00, $CHCl_3$), indicating a normal configuration by comparison to previously reported diterpenes (Suzuki et al., 1983). Given that KgTS does not alter the decalin ring core structure, this further indicates that the DTC product has the same C9 and C10 configuration as normal CPP (**3**). Accordingly, the SsSS product is (9*R*, 10*S*)-labda-7,14-dien-13-ol (**31**), which has been previously reported (Carman et al., 1973), and the KgTS product is (9*R*,10*S*)-labda-7,13(16),14-triene (**32**), which also has been previously reported (Maskovic et al., 2013). However, biosynthetic routes to **31** and **32** were not previously known. Their mass spectra can be found in the Supporting Information (Fig. S14).

In the case of the only known DTC that produces peregrinol diphosphate (**11**) the stereochemical configuration of the C8-methyl has not yet been defined (Zerbe et al., 2014). Again, both SsSS and KgTS readily react with **11**, enabling purification of sufficient amounts for full structural characterization by NMR (Figs S15 – S18 and Tables S4 & S5). In addition to establishing the positions of the introduced hydroxyl group in the SsSS product and the carbon-carbon double bond in the KgTS product, it was possible to use the observed NOESY correlations to determine that the C8-methyl was in the α or *R* configuration. Under the assumption that this arrangement is retained from the DTC product, this configuration is consistent with that observed in the derived diterpenoid marrubiin, and presumably stems from a *pro*-chair-boat conformation of **1** prior to bicyclization that leads to an initial *syn*-labda-13*E*-en-8-yl$^+$ intermediate that undergoes a C9 → C8 hydride transfer before termination via the addition of water to the resulting 9-yl$^+$ and deprotonation (Fig. 4). Hence, it was recognized that the SsSS product corresponds to the previously reported diterpenoid viteagnusin D (**33**)(Ono et al., 2008), while KgTS produces the novel diterpene (8*R*,9*R*,10*S*)-labda-13(16),14-dien-9-ol (**34**). Again, biosynthetic routes to **33** and **34** were not previously known. Their mass spectra can be found in the Supporting Information (Fig. S19).

Both SsSS and KgTS readily react with *ent*-kolavenyl diphosphate (**12**). Purification and structural characterization of both compounds by NMR (Figs S20 – S23 and Tables S6 &

S7) revealed that SsSS removes the diphosphate and forms a tertiary alcohol, *ent*-kolavelool (**35**)(Soares et al., 2014), while KgTS removes the diphosphate and forms an additional carbon-carbon double bond, producing the *exo*-methylene containing (5*R*,8*R*,9*S*,10*R*)-cleroda-3,13(16),14-triene (**36**), which has been previously observed (Nagashima et al., 1998). Notably, SsSS and KgTS also readily react with kolavenyl diphosphate (**13**) resulting in enantiomeric products to those observed with **12**, as indicated by their identical retention times and mass spectra upon non-chiral GC-MS analysis (Fig. S24). Thus, with **13** SsSS produces the known diterpenoid kolavelool (**37**)(Misra et al., 1979), which also has been reported to be produced from **13** by a DTS found in the same operon as the relevant DTC (Nakano et al., 2015), while KgTS produces a new enzymatic product (5*S*,8*S*,9*R*,10*S*)-cleroda-3,13(16),14-triene (**38**). Similarly, with the enantiomer of its native substrate, SsSS produces the enantiomer of its usual product, again as indicated by their identical retention times and mass spectra upon non-chiral GC-MS analysis (Fig. S25) – i.e., from **8** SsSS produces *ent*-sclareol (**39**). Other than for **37**, biosynthetic routes were not previously known for these diterpenes (i.e., **35**, **36**, **38** & **39**).

Both SsSS and KgTS further readily react with *syn*-halimadienyl diphosphate (**14**), with some overlap in product profile as KgTS yields small amounts of the same product observed with SsSS. Purification and structural characterization of both compounds by NMR revealed that these catalyze their prototypical reactions (Figs S26 – S29 and Tables S8 & S9). SsSS forms the C13 tertiary alcohol, (8*R*,9*R*,10*S*)-halimada-5,14-dien-13-ol (**40**), while KgTS forms the corresponding *exo*-methylene derivative, (8*R*,9*R*,10*S*)-halimada-5,13(16),14-triene (**41**). Both **40** and **41** appear to be novel diterpenes and, accordingly, biosynthetic routes to these were not previously known. Their mass spectra can be found in the Supporting Information (Fig. S30).

KgTS also reacts with **7** to produce two compounds. While the minor component was identified as *cis*-abienol (**26**), it was necessary to purify the major product and carry out NMR analysis (Figs S31 & S32 and Table S10), which led to its assignment as the known diterpenoid *iso*-abienol (**42**)(Ekman et al., 1977). Not surprisingly, this results from removal of the diphosphate and formation of the C13 *exo*-methylene (i.e., a 13(16) double bond). Finally, SsSS reacts with **9** to produce an unknown product that also was purified and structurally characterized by NMR (Figs S33 & S34 and Table S11), again a result of removal of the diphosphate and formation of a C13 hydroxyl group, yielding the novel diterpene (5*S*,8*R*,9*R*,10*S*)-cleroda-3,14-dien-13-ol (**43**). Its mass spectra can be found in Fig. 4 (panel L). Yet again, biosynthetic routes to **42** and **43** were not previously known. Their mass spectra can be found in the Supporting Information (Fig. S35).

For ease of reference, all the SsSS and KgTS products reported here (i.e., **15** – **43**) are listed in Table 2. Also presented in addition to the common name of the product (where available) are the corresponding semi-systematic names. These are derived from the three basic skeletal structures of DTC products, along with the stereochemical descriptor assigned to the common labdadienyl$^+$ diphosphate intermediate in the catalyzed reaction, as defined in Fig. 1.

3. Discussion

Combinatorial biosynthesis can be most readily envisioned with the availability of enzymes that exhibit significant substrate promiscuity. In this study, taking advantage of a previously developed modular metabolic engineering system, it was possible to demonstrate a striking degree of promiscuity for both the bacterial DTS, KgTS, and plant DTS, SsSS, which both reacted with all 12 bicyclic DTC products tested here (Fig. 3). This includes not only all three available stereoisomers of CPP (**3 – 5**), but also analogs with an alternative double bond (**6**) and where hydroxyl groups are present (**7**, **8** & **11**), as well as rearranged backbones, both of the halimadane (**10** & **14**) or clerodane (**9**, **12** & **13**) types in various configurations (Fig. 1). In addition, both will react with the upstream *transoid* acyclic precursor **1**, with SsSS further capable of reacting to some extent with the acyclic *cisoid* analog **2**, although neither DTS competes efficiently with the DTCs utilized here for **1**. Hence, both SsSS and KgTS seem to readily react with C_{20} isoprenyl precursors with *trans* configuration of the carbon-carbon double bond allylic to the diphosphate ester linkage (Fig. 5). Notably, their ability to do so has already proven useful in resolution of the stereochemistry of previously incompletely defined DTC products (i.e., **6** & **11**), and it is expected that these will be useful for future characterization of DTCs that catalyze novel product outcome.

Notably, SsSS and KgTS are functionally distinct, predominantly producing different products from the same substrates. As with all terpene synthases in general, these two DTSs catalyze heterolytic cleavage of the allylic diphosphate ester bond in their substrate, forming an allylic carbocation that is localized to the tertiary position, whereupon their activity diverges, each representing one of the two primary means by which terpene synthases terminate their reactions. In particular, KgTS seems to almost invariably directly quench this 13-yl$^+$ intermediate by deprotonation, generally at the neighboring methyl group, yielding a product with a newly formed *exo*-methylene moiety. This is the prototypical olefin generating terpene synthase reaction. On the other hand, SsSS seems to invariably first add a water to the 13-yl$^+$ intermediate before quenching the resulting oxacarbenium ion by deprotonation to yield a 13-hydroxy product. While less common, this type of reaction is catalyzed by a number of terpene synthases.

In order to carry out cyclization, terpene synthases must position a distal carbon-carbon double bond for addition to the allylic carbocation generated by lysis of the diphosphate ester bond in their substrate, which requires interaction beyond the proximal isoprenyl unit. By contrast, SsSS and KgTS generally do not catalyze cyclization, alleviating any such requirement for extended interaction with their substrate beyond the diphosphate and directly coupled isoprenyl unit (i.e., that shown in Fig. 5), which presumably underlies their extreme promiscuity. Conversely, this suggests that cyclases will be more constrained and exhibit less promiscuity. Indeed, previous investigations have shown only limited promiscuity for such DTSs, observing effective activity with at most two different stereoisomers of CPP (Morrone et al., 2011; Zhou et al., 2012), or 8-hydroxy-CPP with the same stereoconfiguration as their native substrate (Mafu et al., 2015).

Perhaps more importantly, the distinct activity of SsSS and KgTS, coupled to their extreme promiscuity, provides access to two distinct derivatives of a wide range of DTC products (Fig. 6; see Table 2 for full listing with semi-systematic nomenclature). Of particular note, while the combined action of DTCs and DTSs prototypically produce highly hydrophobic diterpene olefins, use of SsSS in conjunction with a DTC that yields a hydroxylated bicycle (e.g., **7**, **8** & **11**), directly produces di-hydroxylated products (e.g., **19**, **39** & **33**, respectively), the spatially separated hydroxyl groups of which not only add hydrogen-bonding capacity, but also significantly increase the solubility and, altogether, the corresponding potential for biological activity of the resulting diterpenoids.

Despite the lack of any substantial effort towards optimization of the DTC/DTS combinations examined here (e.g., balancing their expression levels), almost all pairings exhibited efficient production of the resulting diterpene, almost invariably >90% conversion of the DTC product, with yields of up to 15 mg/L. This enabled ready purification of enough of these compounds for structural determination by NMR analysis and optical rotation measurement, which enabled structural characterization of the 13 unknown products (i.e., **31** – **43**). In addition, these pairings further provide sufficient material for exploration of potential subsequently acting enzymes such as cytochrome P450 mono-oxygenases, which also can be incorporated into this modular metabolic engineering system (Kitaoka et al., 2015). For example, it has recently been shown that the kaurene oxidase from gibberellin plant hormone biosynthesis in *Arabidopsis thaliana* exhibits a remarkable degree of promiscuity (Mafu et al., 2016), and the results reported here significantly expand the range of labdane-related diterpenes that can be explored in such studies.

1. Conclusions

In summary, the extreme promiscuity shown here for the functionally orthogonal SsSS and KgTS enables true combinatorial labdane-related diterpene biosynthesis (Figs. 5 & 6), with the production of at least two distinct diterpenes from any DTC product (i.e., the tertiary alcohol typically generated by SsSS and the *exo*-methylene olefin typically generated by KgTS). Notably, 5 of these products appear to be novel diterpenes that have not been previously observed (i.e., **34**, **38**, **40**, **41**, & **43**). Moreover, this further provides a basis for biotechnological access to the diterpenes reported here, such *cis*-abienol and sclareol, which already have proven industrial value (Caniard et al., 2012; Sallaud et al., 2012; Schalk et al., 2012; Zerbe et al., 2012), as well as those that can be generated by SsSS and KgTS from the range of potential DTC products for which relevant enzymes have yet to be discovered. Indeed, the results reported here already provided biosynthetic routes to 12 previously inaccessible diterpenes (i.e., **31** – **36** & **38** – **43**), as well as 4 others for which efficient enzymatic production had not yet been reported (i.e., **27** – **30**)[2]. In addition, the strong flux observed with these promiscuous DTSs not only provides immediate access to their

[2]While this manuscript was under review, a study with some overlap to the results reported here was published (Andersen-Ranberg et al., 2016). In particular, the ability of SsSS to react with 7 DTC products (**3** – **5**, **7**, **8**, **11** & **12**), with observation of the same products (**21**, **28**, **29**, **19**, **39**, **33** & **35**, respectively), although **33** was not structurally characterized. Moreover, the promiscuity of SsSS was used to help characterize a novel DTC, aiding elucidation of its product as **12**. In addition, while no work was reported with KgTS, the same *ent*-manoyl oxide (**27**) product from **8** was reported with another DTS.

immediate products, but potentially also derived diterpenoid natural products, enabling investigation of their possible industrial uses.

5. Methods and Materials

5.1. General

Unless otherwise noted, chemicals were purchased from Fisher Scientific and molecular biology reagents, including synthetic genes, from Invitrogen. The vectors used here are described in Table S2. All constructs were verified by full sequencing of the inserted gene. Authentic standards were obtained for sclareol (Aldrich) and geranyllinalool [gift from Prof. Dorothea Tholl, Virginia Tech (Herde et al., 2008)]. Other diterpenes were identified by comparison to known products of other DTSs, which were also utilized here, as described below.

5.2. Recombinant constructs

The modularity of the metabolic system utilized here is based on the use of DEST cassettes that enable facile recombination via the Gateway cloning system (Invitrogen). Accordingly, all the DTCs and DTSs were first cloned into a pENTR/SD/D-TOPO vector. While genes for many of the DTCs were already available from previous work (see Table 1), in a number of cases (Haur_2145 and MvCPS1, as well as for SsSS as a pseudo-mature construct without the N-terminal plastid targeting sequence), these were obtained by gene synthesis, with codon optimization for expression in *E. coli*, and the corresponding gene sequences can be found in the Supplemental Information document. KgTS and KgTPS were cloned from *Kitasatospora griseola*, obtained from RIKEN-BRC, while the Rv3378c used for product identification was a previously described clone from *Mycobacterium tuberculosis* (Mann et al., 2009b). As previously reported (Cyr et al., 2007), the production of **1** relies on a GGPP synthase expressed from a pACYCDuet (Novagen) based expression vector, pGG, which also has been further modified with the addition of a DEST cassette, pGG-DEST, into which the DTCs utilized here were recombined from pENTR/SD/D-TOPO vectors. The DTSs were recombined into the compatible pDEST14 expression vector. Due to poor expression from the relevant pGG-DEST::DTC construct with the terpentedienyl diphosphate synthase (KgTPS), this DTC was recombined into pDEST14, with the DTSs then recombined into pGG-DEST instead. Production of **2** was accomplished with a previously reported NNPP synthase expression vector (Zi et al., 2014b), which was further modified by insertion of a DEST cassette into which SsSS and KgTS were recombined. To increase metabolic flux towards terpenoids, several key genes from the endogenous isoprenoid precursor pathway were over-expressed using the previously reported pIRS construct (Morrone et al., 2010), which also is compatible with all the vectors described above.

5.3. Metabolic Engineering

All metabolic engineering was carried out using the *E. coli* OverExpress C41 strain (Lucigen), and included pIRS as well as the relevant expression constructs (i.e., for the production of **1** or **2**, and a DTC and/or DTS). For initial activity screening purpose, recombinant cultures were grown in 50 mL TB medium (pH = 7.0), with appropriate antibiotics, in 250 mL Erlenmeyer flasks. These cultures were first grown at 37 °C to mid-

log phase (OD_{600} ~0.7), then the temperature dropped to 16 °C for 0.5 h prior to induction with 1 mM isopropylthiogalactoside (IPTG) and supplementation with 40 mM pyruvate and 1 mM $MgCl_2$. The induced cultures were grown for an additional 72 h before extraction with an equal volume of hexanes, with the organic phase then separated, and concentrated under N_2 when necessary.

5.4. Diterpene product analysis by GC-MS chromatography

Gas chromatography with mass spectral detection was carried on a Varian 3900 GC with a Saturn 2100T ion trap mass spectrometer in electron ionization (70 eV) mode, using an Agilent HP-5MS column (Agilent, 19091S-433) with 1.2 mL/min helium flow rate. Samples (1 uL) were injected in splitless mode by an 8400 autosampler with the injection port at 250 °C. The following temperature program was used: the column oven temperature initially started at 50 °C, which was maintained for 3 min, and then increased at a rate of 15 °C/min to 300 °C, where it was held for another 3 min. Mass spectrum was recorded by mass-to-charge ratio (*m/z*) values in a range from 90 to 650, starting from 13 min after sample injection until the end of the run. As previously noted (Sallaud et al., 2012; Zerbe et al., 2012), *cis*-abienol (**29**) is thermally labile, necessitating injection at a lower temperature (80 °C) and a slower temperature ramp for the column oven (starting at 40 °C, immediately rising 10 °C/min to 100 °C and then 3 °C/min to 240 °C, where it was held for 3 min), which were utilized for GC-MS analysis of this compound (i.e., Fig. 3 and S5).

5.5. Diterpene production and purification

To obtain sufficient amount of new enzymatic products for NMR analysis, the bacterial cultures described above were simply scaled up to 1 L in 2.8 L Fernbach flasks. All other procedures were identical except that the extraction was repeated twice to ensure full yield. The pooled separated organic phase was dried by rotary evaporation under vacuum, and the residue was re-suspended in 5 mL hexane for subsequent fractionation via flash chromatography over a 4 g-silica column (Grace) using a Grace Reveleris flash chromatography system with UV detection and automated injector and fraction collector, run at 15 mL/min. Briefly, the column was pre-equilibrated with hexanes and the sample injected, followed by 100% hexane (0–4 min), 0–100% acetone (4–5 min), 100% acetone (5–8 min), with peak-based fraction collection (15 mL maximum per tube). Generally, non-oxygen containing products would come out in the 100% hexane fraction; otherwise, the products eluted in 100% acetone fractions. Fractions of interest were dried under N_2, re-suspended in 2 mL methanol, and filtered through 0.2 um cellulose filter (Thermo scientific). These fractions were further separated using an Agilent 1200 series HPLC instrument equipped with a diode array UV detector and automated injector and fraction collector, over a semi-preparative C-8 column (ZORBAX Eclipse XDB-C8, 25 × 0.94 cm) run at 4 mL/min. The column was pre-equilibrated with acetonitrile/water (1:1 for olefins, 4:1 for oxygenated products), the sample injected, followed by washing (0–2 min) with same acetonitrile/water mix (i.e., depending on the targeted compound), then the percentage of acetonitrile increased to 100% (2–10 min), and final elution with 100% acetonitrile (10–30 min), with collection of 0.5 mL fractions. Fractions were analyzed by GC-MS and, if necessary, compounds were further purified by another round of HPLC separation over an analytical C-8 column (Kromasil® C8, 50 × 4.6 mm) run at 0.5 mL/min, and using the same

elution program described above. Fractions containing pure compounds were dried under N_2, and the compounds then dissolved in 0.5 mL deuterated solvents for NMR analysis.

5.6. Chemical structure identification by NMR analysis

Samples were dried under N_2 and dissolved in 0.5 mL deuterated solvents, generally $CDCl_3$ (Aldrich), except with compounds **33** and **34**, which were dissolved in C_6D_6 (Aldrich). NMR spectra were acquired on a Bruker AVIII-800 spectrometer equipped with a 5-mm HCN cryogenic probe, using TopSpin 3.2 software. Analysis was carried out at 25 °C except for compounds **40** and **41**, for which the temperature was increased to 50 °C in order to increase peak resolution. Chemical shifts were calculated by reference to those known for $CDCl_3$ (^{13}C 77.23 ppm, ^{1}H 7.24 ppm) or C_6D_6 (^{13}C 128.39 ppm, ^{1}H 7.16 ppm) signals offset from TMS. All spectra were acquired using standard programs from the TopSpin 3.2 software, with collection of 1D ^{1}H-NMR, and 2D double-quantum filtered correlation spectroscopy (DQF-COSY), heteronuclear single-quantum coherence (HSQC), heteronuclear multiple-bond correlation (HMBC), HMQC-COSY and NOESY (800 MHz), as well as 1D ^{13}C-NMR (201 MHz) spectra. Observed HMBC correlations were used to propose a partial structure, while COSY correlations between protonated carbons were used to complete the structure, which was further verified by HSQC correlations. Observed correlations from NOESY spectrum were used to assign the relative stereochemistry of chiral carbons and also the configuration of double bonds, where applicable.

5.7. Chemical structure identification by optical rotation measurement

To investigate the absolute configuration of compounds **32** and **35**, their optical rotations were measured in $CHCl_3$ solvent on an AP-300 automatic polarimeter (ATAGO) at 25 °C. These measurements were carried out according to the instruction manual, in particular using mode 1 with tube E (50 mm). The instrument was blanked with pure solvent, and 5 readings for each sample were recorded and the average value reported here.

Supplementary Material

Refer to Web version on PubMed Central for supplementary material.

Acknowledgments

This work was supported by a grant from the NIH (GM109773 to R.J.P.).

References

Andersen-Ranberg J, Kongstad KT, Nielsen MT, Jensen NB, Pateraki I, Bach SS, Hamberger B, Zerbe P, Staerk D, Bohlmann J, Moller BL, Hamberger B. Expanding the Landscape of Diterpene Structural Diversity through Stereochemically Controlled Combinatorial Biosynthesis. Angew Chem Int Ed Engl. 2016; 55:2142–6. [PubMed: 26749264]

Caniard A, Zerbe P, Legrand S, Cohade A, Valot N, Magnard JL, Bohlmann J, Legendre L. Discovery and functional characterization of two diterpene synthases for sclareol biosynthesis in *Salvia sclarea* (L.) and their relevance for perfume manufacture. BMC Plant Biol. 2012; 12:119. [PubMed: 22834731]

Carman RM, Craig WJ, Shaw IM. Diterpenoids. XXXII. Labda-8,14-dien-13β-ol. Aust J Chem. 1973; 26:215–217.

Criswell J, Potter K, Shephard F, Beale MH, Peters RJ. A single residue change leads to a hydroxylated product from the class II diterpene cyclization catalyzed by abietadiene synthase. Organic letters. 2012; 14:5828–31. [PubMed: 23167845]

Croteau R, Ketchum RE, Long RM, Kaspera R, Wildung MR. Taxol biosynthesis and molecular genetics. Phytochem Rev. 2006; 5:75–97. [PubMed: 20622989]

Cui G, Duan L, Jin B, Qian J, Xue Z, Shen G, Snyder JH, Song J, Chen S, Huang L, Peters RJ, Qi X. Funcation divergence of diterpene synthases in the medicinal plant *Salvia miltiorrhiza* Bunge. Plant Physiol. 2015; 169:1607–1618. [PubMed: 26077765]

Cyr A, Wilderman PR, Determan M, Peters RJ. A Modular Approach for Facile Biosynthesis of Labdane-Related Diterpenes. J Am Chem Soc. 2007; 129:6684–6685. [PubMed: 17480080]

Dairi T, Hamano Y, Kuzuyama Y, Itoh N, Furihata K, Seto H. Eubacterial diterpene cyclase genes essential for production of the isoprenoid antibiotic terpentecin. J Bact. 2001; 183:6085–6092. [PubMed: 11567009]

Ekman R, Sjöholm R, Hannus K. Isoabienol, the principal diterpene alcohol in *Pinus sylvestris* needles. Acta Chem Scand. 1977; 31:921–922.

Falara V, Pichersky E, Kanellis AK. A copal-8-ol diphosphate synthase from the angiosperm *Cistus creticus* subsp. *creticus* is a putative key enzyme for the formation of pharmacologically active, oxygen-containing labdane-type diterpenes. Plant Physiol. 2010; 154:301–10. [PubMed: 20595348]

Gao W, Hillwig ML, Huang L, Cui G, Wang X, Kong J, Yang B, Peters RJ. A functional genomics approach to tanshinone biosynthesis provides stereochemical insights. Org Lett. 2009; 11:5170–5173. [PubMed: 19905026]

Guo J, Ma X, Cai Y, Ma Y, Zhan Z, Zhou YJ, Liu W, Guan M, Yang J, Cui G, Kang L, Yang L, Shen Y, Tang J, Lin H, Ma X, Jin B, Liu Z, Peters RJ, Zhao ZK, Huang L. Cytochrome P450 promiscuity leads to a bifurcating biosynthetic pathway for tanshinones. New Phytol. in press.

Hamano Y, Kuzuyama Y, Itoh N, Furihata K, Seto H, Dairi T. Functional analysis of eubacterial diterpene cyclases responsible for biosynthesis of a diterpene antibiotic, terpentecin. J Biol Chem. 2002; 277:37098–37104. [PubMed: 12138123]

Harris LJ, Saparno A, Johnston A, Prisic S, Xu M, Allard S, Kathiresan A, Ouellet T, Peters RJ. The maize An2 gene is induced by Fusarium attack and encodes an ent-copalyl diphosphate synthase. Plant Mol Biol. 2005; 59:881–894. [PubMed: 16307364]

Herde M, Gartner K, Kollner TG, Fode B, Boland W, Gershenzon J, Gatz C, Tholl D. Identification and regulation of TPS04/GES, an *Arabidopsis* geranyllinalool synthase catalyzing the first step in the formation of the insect-induced volatile C16-homoterpene TMTT. Plant Cell. 2008; 20:1152–68. [PubMed: 18398052]

Hershey DM, Lu X, Zi J, Peters RJ. Functional conservation of the capacity for *ent*-kaurene biosynthesis and an associated operon in certain rhizobia. J Bact. 2014; 196:100–106. [PubMed: 24142247]

Hoshino T, Nakano C, Ootsuka T, Shinohara Y, Hara T. Substrate specificity of Rv3378c, an enzyme from Mycobacterium tuberculosis, and the inhibitory activity of the bicyclic diterpenoids against macrophage phagocytosis. Organic & biomolecular chemistry. 2011; 9:2156–65. [PubMed: 21290071]

Ignea C, Ioannou E, Georgantea P, Loupassaki S, Trikka FA, Kanellis AK, Makris AM, Roussis V, Kampranis SC. Reconstructing the chemical diversity of labdane-type diterpene biosynthesis in yeast. Metabolic engineering. 2015; 28:91–103. [PubMed: 25498547]

Jackson AJ, Hershey DM, Chesnut T, Xu M, Peters RJ. Biochemical characterization of the castor bean *ent*-kaurene synthase(-like) family supports quantum chemical view of diterpene cyclization. Phytochemistry. 2014; 103:13–21. [PubMed: 24810014]

Kato-Noguchi H, Peters RJ. The role of momilactones in rice allelopathy. J Chem Ecol. 2013; 39:175–185. [PubMed: 23385366]

Kitaoka N, Lu X, Yang B, Peters RJ. The application of synthetic biology to elucidation of plant mono-, sesqui-, and diterpenoid metabolism. Mol Plant. 2015; 8:6–16. [PubMed: 25578268]

Layre E, Lee HJ, Young DC, Martinot AJ, Buter J, Minnaard AJ, Annand JW, Fortune SM, Snider BB, Matsunaga I, Rubin EJ, Alber T, Moody DB. Molecular profiling of Mycobacterium tuberculosis

identifies tuberculosinyl nucleoside products of the virulence-associated enzyme Rv3378c. Proc Natl Acad Sci U S A. 2014; 111:2978–83. [PubMed: 24516143]

Lu X, Hershey DM, Wang L, Bogdanove AJ, Peters RJ. An *ent*-kaurene derived diterpenoid virulence factor from *Xanthomonas oryzae* pv. oryzicola. New Phytol. 2015; 406:295–302. [PubMed: 25406717]

Mafu S, Hillwig ML, Peters RJ. A novel labda-7,13e-dien-15-ol-producing bifunctional diterpene synthase from *Selaginella moellendorffii*. ChemBioChem. 2011; 12:1984–7. [PubMed: 21751328]

Mafu S, Jia M, Zi J, Xu M, Morrone D, Wu Y, Peters RJ. Probing the promiscuity of *ent*-kaurene oxidase via combinatorial biosynthesis. Proc Natl Acad Sci U S A. 2016 in press.

Mafu S, Potter KC, Hillwig ML, Schulte S, Criswell J, Peters RJ. Efficient heterocyclisation by (di)terpene synthases. Chem Commun (Camb). 2015; 51:13485–7. [PubMed: 26214384]

Mann FM, Prisic S, Hu H, Xu M, Coates RM, Peters RJ. Characterization and inhibition of a class II diterpene cyclase from Mycobacterium tuberculosis: implications for tuberculosis. The Journal of biological chemistry. 2009a; 284:23574–9. [PubMed: 19574210]

Mann FM, Xu M, Chen X, Fulton DB, Russell DG, Peters RJ. Edaxadiene: a new bioactive diterpene from *Mycobacterium tuberculosis*. J Am Chem Soc. 2009b; 131:15726–15727.

Maskovic P, Radojkovic M, Ristic M, Solujic S. Studies on the antimicrobial and antioxidant activity and chemical composition of the essential oils of Kitaibelia vitifolia. Nat Prod Commun. 2013; 8:667–670.

Maugel N, Mann FM, Hillwig ML, Peters RJ, Snider BB. Synthesis of (+/−)-nosyberkol (isotuberculosinol, revised structure of edaxadiene) and (+/−)-tuberculosinol. Org Lett. 2010; 12:2626–2629. [PubMed: 20462237]

Misra R, Pandey RC, Dev S. Higher isoprenoids X: Diterpenoids from the oleoresin of *Harwickia pinnata* part 3: kolavenol, klavelool and a nor diterpene hydrocarbon. Tetrahedron. 1979; 35:985–987.

Morrone D, Chambers J, Lowry L, Kim G, Anterola A, Bender K, Peters RJ. Gibberellin biosynthesis in bacteria: Separate *ent*-copalyl diphosphate and *ent*-kaurene synthases in *Bradyrhizobium japonicum*. FEBS Lett. 2009; 583:475–480. [PubMed: 19121310]

Morrone D, Hillwig ML, Mead ME, Lowry L, Fulton DB, Peters RJ. Evident and latent plasticity across the rice diterpene synthase family with potential implications for the evolution of diterpenoid metabolism in the cereals. Biochem J. 2011; 435:589–595. [PubMed: 21323642]

Morrone D, Lowry L, Determan MK, Hershey DM, Xu M, Peters RJ. Increasing diterpene yield with a modular metabolic engineering system in E. coli: comparison of MEV and MEP isoprenoid precursor pathway engineering. Appl Microbiol Biotechnol. 2010; 85:1893–1906. [PubMed: 19777230]

Nagashima F, Takaoka S, Asakawa Y. Diterpenoids from the japanese liverwort Jungermannia infusca. Phytochemistry. 1998; 49:601–608.

Nakano C, Hoshino H, Sato T, Toyomasu T, Dairi T, Sassa T. Substrate specificity of the CYC2 enzyme from *Kitasatospora griseola*: production of sclarene, biformene, and novel bicyclic diterpenes by the enzymatic reactions of labdane-and halimane-type diterpene diphosphates. Tetrahedron Lett. 2010; 51:125–128.

Nakano C, Ootsuka T, Takayama K, Mitsui T, Sato T, Hoshino T. Characterization of the Rv3378c gene product, a new diterpene synthase for producing tuberculosinol and (13R, S)-isotuberculosinol (nosyberkol), from the Mycobacterium tuberculosis H37Rv genome. Bioscience, biotechnology, and biochemistry. 2011; 75:75–81.

Nakano C, Oshima M, Kurashima N, Hoshino T. Identification of a new diterpene biosynthetic gene cluster that produces O-methylkolavelool in Herpetosiphon aurantiacus. Chembiochem : a European journal of chemical biology. 2015; 16:772–81. [PubMed: 25694050]

Noike M, Ambo T, Kikuchi S, Suzuki T, Yamashita S, Takahashi S, Kurokawa H, Mahapatra S, Crick DC, Koyama T. Product chain-length determination mechanism of Z,E-farnesyl diphosphate synthase. Biochem Biophys Res Commun. 2008; 377:17–22. [PubMed: 18790692]

Ono M, Yamasaki T, Konoshita M, Ikeda T, Okawa M, Kinjo J, Yoshimitsu H, Nohara T. Five new diterpenoids, viteagnusins A--E, from the fruit of Vitex agnus-castus. Chem Pharm Bull (Tokyo). 2008; 56:1621–4. [PubMed: 18981619]

Peters RJ. Two rings in them all: The labdane-related diterpenoids. Nat Prod Rep. 2010; 27:1521–1530. [PubMed: 20890488]

Peters RJ, Flory JE, Jetter R, Ravn MM, Lee HJ, Coates RM, Croteau RB. Abietadiene synthase from grand fir (Abies grandis): characterization and mechanism of action of the “pseudomature” recombinant enzyme. Biochemistry. 2000; 39:15592–602. [PubMed: 11112547]

Potter K, Criswell J, Zi J, Stubbs A, Peters RJ. Novel product chemistry from mechanistic analysis of ent-copalyl diphosphate synthases from plant hormone biosynthesis. Angewandte Chemie. 2014; 53:7198–202. [PubMed: 24862907]

Potter KC, Jia M, Hong YJ, Tantillo DJ, Peters RJ. Product rearrangement from altering a single residue in the rice syn-copalyl diphosphate synthase. Org Lett. 2016a; 18:1060–1063. [PubMed: 26878189]

Potter KC, Zi J, Hong YJ, Schulte S, Malchow B, Tantillo DJ, Peters RJ. Blocking Deprotonation with Retention of Aromaticity in a Plant ent-Copalyl Diphosphate Synthase Leads to Product Rearrangement. Angew Chem Int Ed. 2016b; 55:634–638.

Sallaud C, Giacalone C, Topfer R, Goepfert S, Bakaher N, Rosti S, Tissier A. Characterization of two genes for the biosynthesis of the labdane diterpene Z-abienol in tobacco (Nicotiana tabacum) glandular trichomes. Plant J. 2012; 72:1–17. [PubMed: 22672125]

Schalk M, Pastore L, Mirata MA, Khim S, Schouwey M, Deguerry F, Pineda V, Rocci L, Daviet L. Towards a Biosynthetic Route to Sclareol and Amber Odorants. J Am Chem Soc. 2012; 134:18900–18903. [PubMed: 23113661]

Schmelz EA, Huffaker A, Sims JW, Christensen SA, Lu X, Okada K, Peters RJ. Biosynthesis, elicitation and roles of monocot terpenoid phytoalexins. Plant J. 2014; 79:659–678. [PubMed: 24450747]

Shimane M, Ueno Y, Morisaki K, Oogami S, Natsume M, Hayashi K, Nozaki H, Kawaide H. Molecular evolution of the substrate specificity of ent-kaurene synthases to adapt to gibberellin biosynthesis in land plants. Biochem J. 2014; 462:539–46. [PubMed: 24983886]

Soares, AdO; Ferreira, AGL.; Soares, LR.; Corsino, J.; Garcez, FR.; Garcez, WS. Chemical study of leaves of Trichilia silvatica (Meliaceae). Quimica Nova. 2014; 37:1487–1490.

Sun TP. The molecular mechanism and evolution of the GA-GID1-DELLA signaling module in plants. Current biology : CB. 2011; 21:R338–45. [PubMed: 21549956]

Suzuki H, Noma M, Kawashima N. Two labdane diterpenoids from Nicotiana setchellii. Phytochemistry. 1983; 22:1294–1295.

Teufel R, Kaysser L, Villaume MT, Diethelm S, Carbullido MK, Baran PS, Moore BS. One-pot enzymatic synthesis of merochlorin A and B. Angew Chem Int Ed Engl. 2014; 53:11019–22. [PubMed: 25115835]

Wu Y, Zhou K, Toyomasu T, Sugawara C, Oku M, Abe S, Usui M, Mitsuhashi W, Chono M, Chandler PM, Peters RJ. Functional characterization of wheat copalyl diphosphate synthases elucidates the early evolution of labdane-related diterpenoid metabolism in the cereals. Phytochemistry. 2012; 84:40–46. [PubMed: 23009878]

Xu M, Hillwig ML, Lane AL, Tiernan MS, Moore BS, Peters RJ. Characterization of an orphan diterpenoid biosynthetic operon from Salinispora arenicola. Journal of natural products. 2014; 77:2144–7. [PubMed: 25203741]

Xu M, Hillwig ML, Prisic S, Coates RM, Peters RJ. Functional identification of rice syn-copalyl diphosphate synthase and its role in initiating biosynthesis of diterpenoid phytoalexin/allelopathic natural products. The Plant journal : for cell and molecular biology. 2004; 39:309–18. [PubMed: 15255861]

Zerbe P, Bohlmann J. Plant diterpene synthases: exploring modularity and metabolic diversity for bioengineering. Trends in biotechnology. 2015; 33:419–28. [PubMed: 26003209]

Zerbe P, Chiang A, Dullat H, O’Neil-Johnson M, Starks C, Hamberger B, Bohlmann J. Diterpene synthases of the biosynthetic system of medicinally active diterpenoids in Marrubium vulgare. Plant J. 2014; 79:914–27. [PubMed: 24990389]

Zerbe P, Chiang A, Yuen M, Hamberger B, Draper JA, Britton R, Bohlmann J. Bifunctional *cis*-abienol synthase from *Abies balsamea* discovered by transcriptome sequencing and its implications for diterpenoid fragrance production. J Biol Chem. 2012; 287:12121–31. [PubMed: 22337889]

Zhou K, Xu M, Tiernan MS, Xie Q, Toyomasu T, Sugawara C, Oku M, Usui M, Mitsuhashi W, Chono M, Chandler PM, Peters RJ. Functional characterization of wheat ent-kaurene(-like) synthases indicates continuing evolution of labdane-related diterpenoid metabolism in the cereals. Phytochemistry. 2012; 84:47–55. [PubMed: 23009879]

Zi J, Mafu S, Peters RJ. To Gibberellins and Beyond! Surveying the Evolution of (Di)Terpenoid Metabolism. Annu Rev Plant Biol. 2014a; 65:259–286. [PubMed: 24471837]

Zi J, Matsuba Y, Hong Y, Jackson A, Pichersky E, Tantillo DJ, Peters RJ. Biosynthesis of lycosantalonol, a *cis*-prenyl derived diterpenoid. J Am Chem Soc. 2014b; 136:16951–16953. [PubMed: 25406026]

Highlights

1. Broad screening of class I diterpene synthase (DTS) activity towards a significant range of structurally diverse potential substrates, many produced by class II diterpene cyclases (DTCs).
2. Extreme promiscuity revealed for a bacterial and, surprisingly, also a plant DTS, enabling combinatorial biosynthesis with considerable yields, enabling structural elucidation of unknown and previously ambiguous structures.
3. Extension of the available diterpene library with the elucidation of 16 new diterpene synthase products.

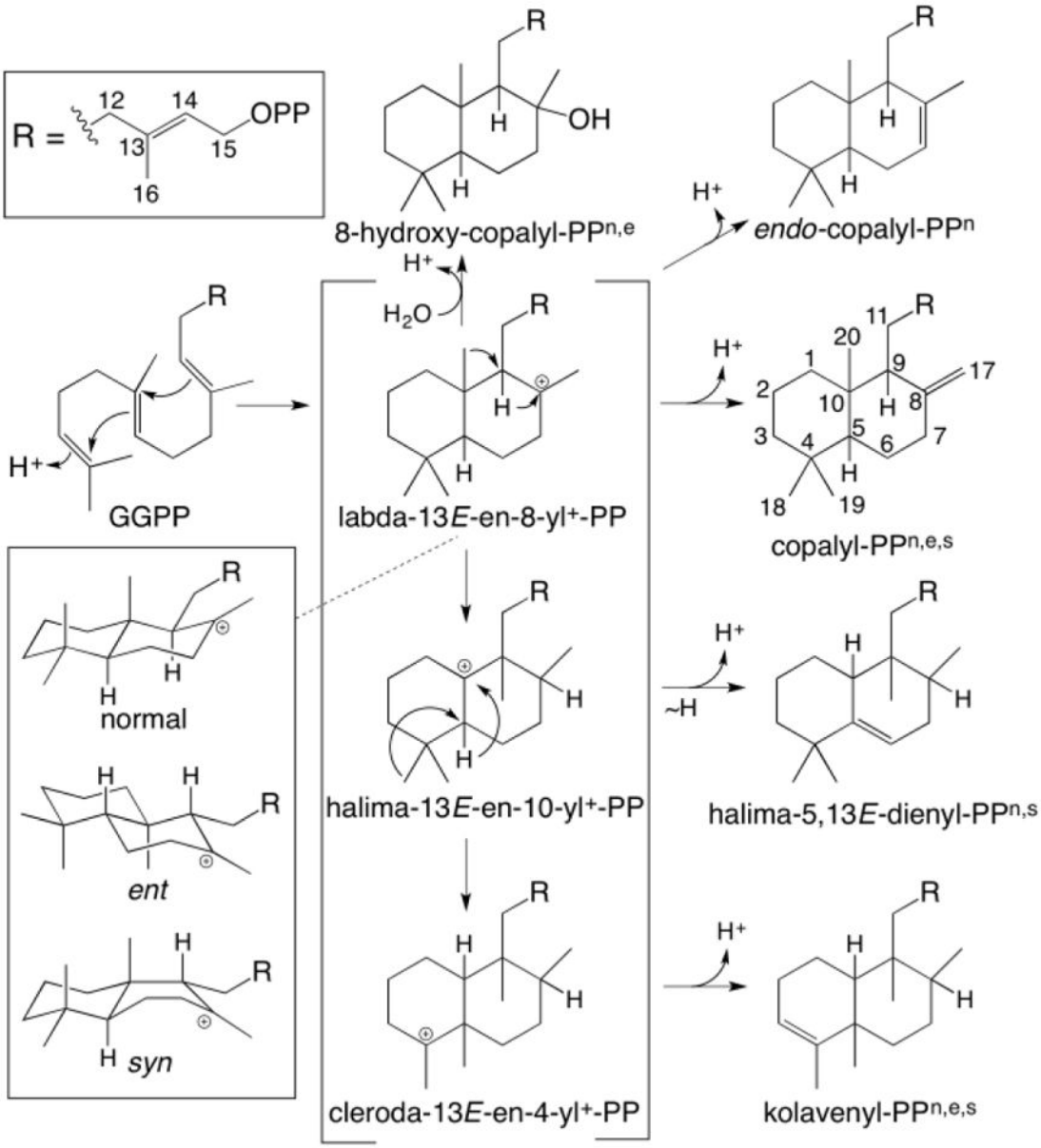

Fig. 1.

Basic DTC products from bicyclization and subsequent rearrangement (PP = diphosphate). Also shown are known stereoisomers for the initial bicycle, and derived products for which DTCs are known are shown by superscript ([n]normal, [e]*ent*, [s]*syn*).

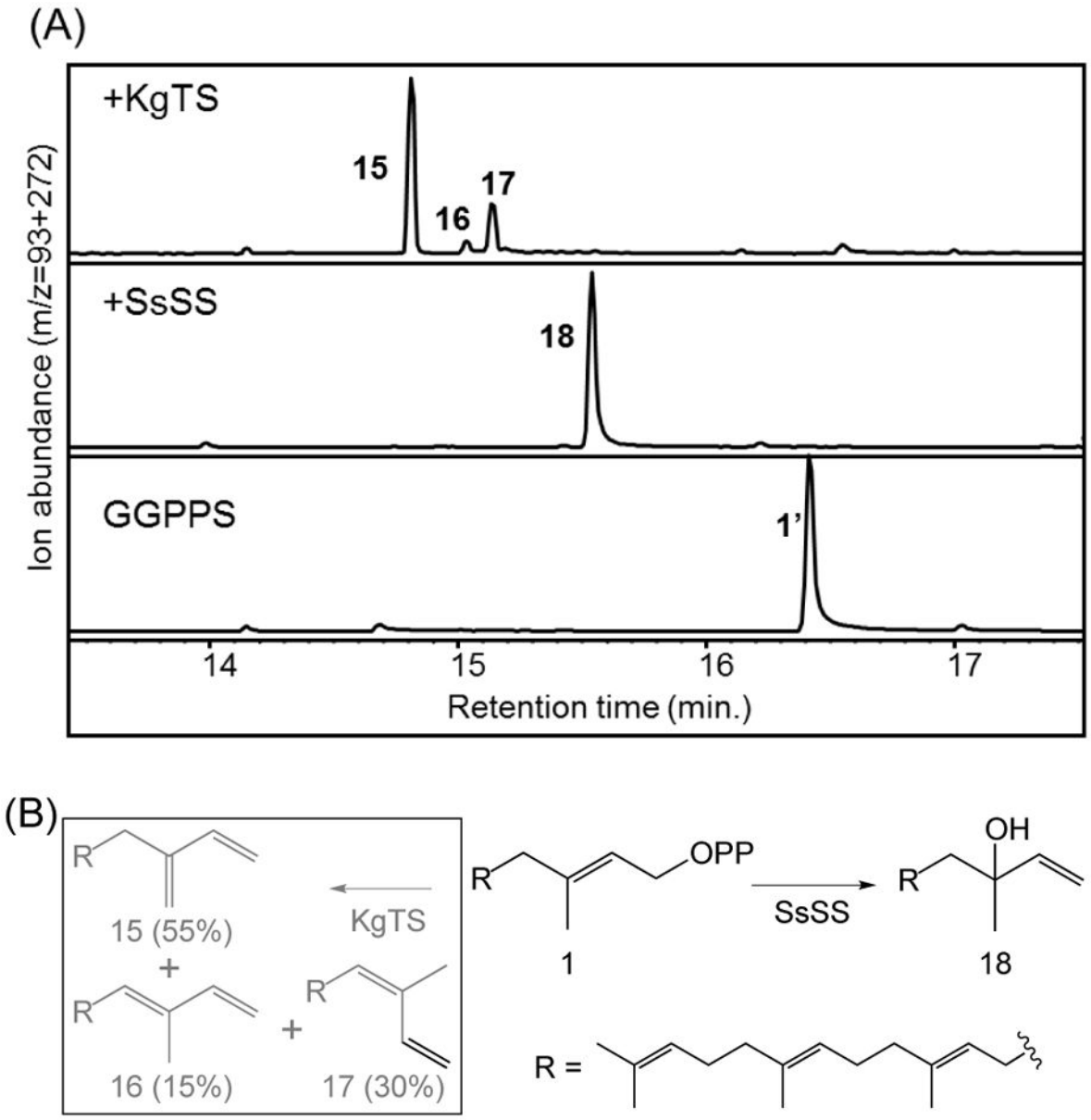

Fig. 2.

SsSS and KgTS readily react with **1**. (A) GC-MS chromatograms of extracts from *E. coli* engineered for production of GGPP (**1**) and expressing either KgTS or SsSS (numbers correspond to chemical structures defined in text, with prime' notation used to indicate the dephosphorylated derivative, where relevant). (B) Reactions catalyzed by KgTS and SsSS with GGPP (**1**). The KgTS reaction arrow and products are shown in gray and boxed, with product ratio shown in parentheses, while the SsSS reaction arrow and product are shown in black.

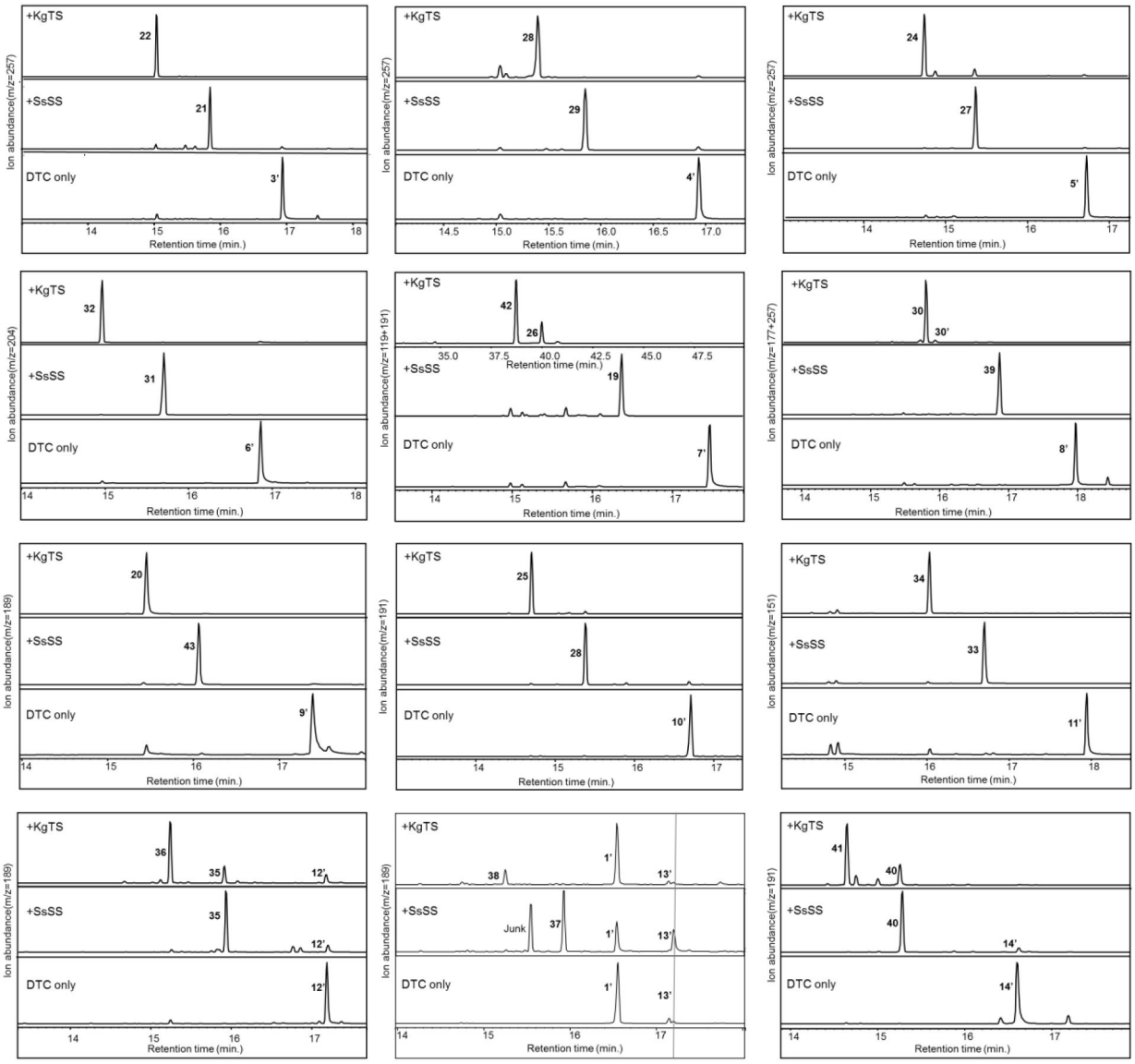

Fig. 3.

GC-MS chromatograms of extracts from *E. coli* engineered for production of one of the 12 distinct DTC products that are currently accessible (**3** – **14**) by introducing a relevant DTC (Table 1) into *E. coli* engineered to produce **1**. The ability of KgTS and SsSS to react with these is demonstrated by their additional co-expression, as indicated in the corresponding chromatograms (numbers correspond to chemical structures defined in text, with prime' notation used to indicate the dephosphorylated derivative, where relevant).

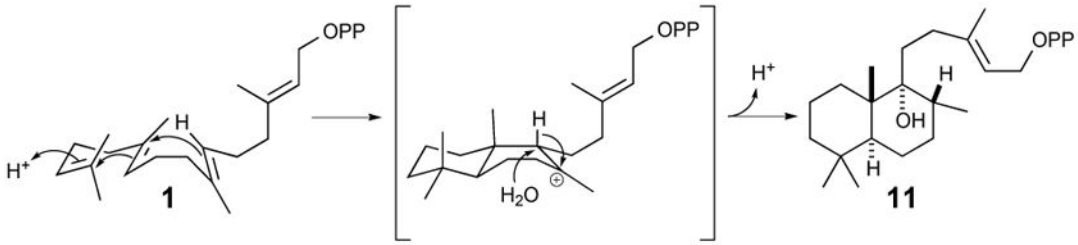

Fig. 4.

Scheme depicting cyclization of **1** to peregrinol diphosphate (**11**). With elucidation of the C8α-methyl conformation reported here, it can be appreciated that this derives from a *pro*-chair-boat conformation of **1** that leads to an initial *syn*-labda-13*E*-en-8-yl$^+$ intermediate, which undergoes a C9 → C8 hydride transfer and addition of water to the resulting 9-yl carbocation before terminating deprotonation.

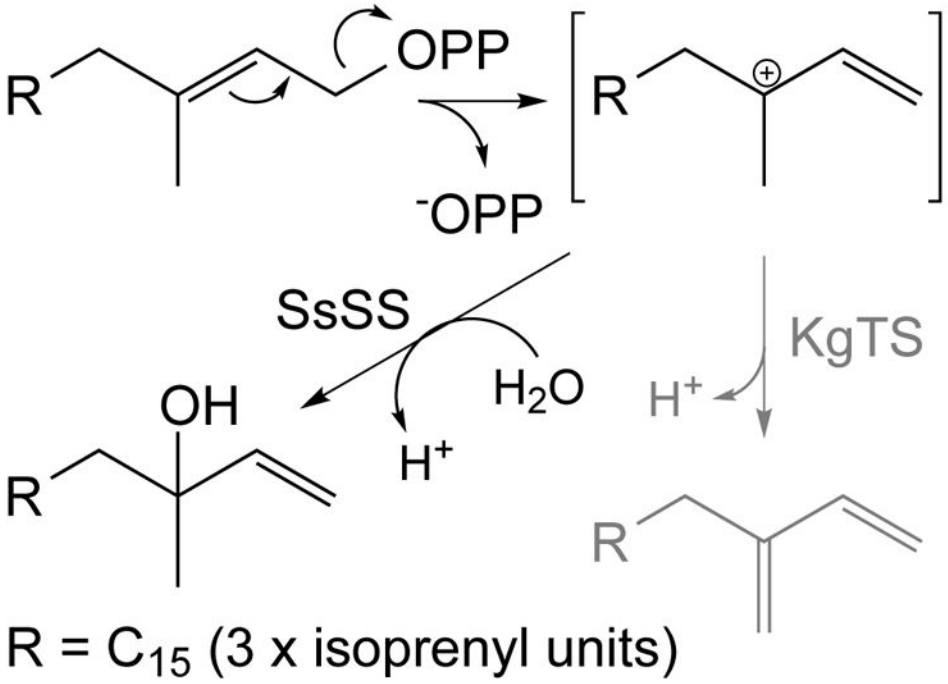

Fig. 5.

Prototypical reactions catalyzed by KgTS (gray arrow and product) or SsSS (black arrow and product) with various diterpene precursors, either **1** or DTC products, via lysis/ionization of the *trans* allylic diphosphate ester to a common tertiary carbocation intermediate.

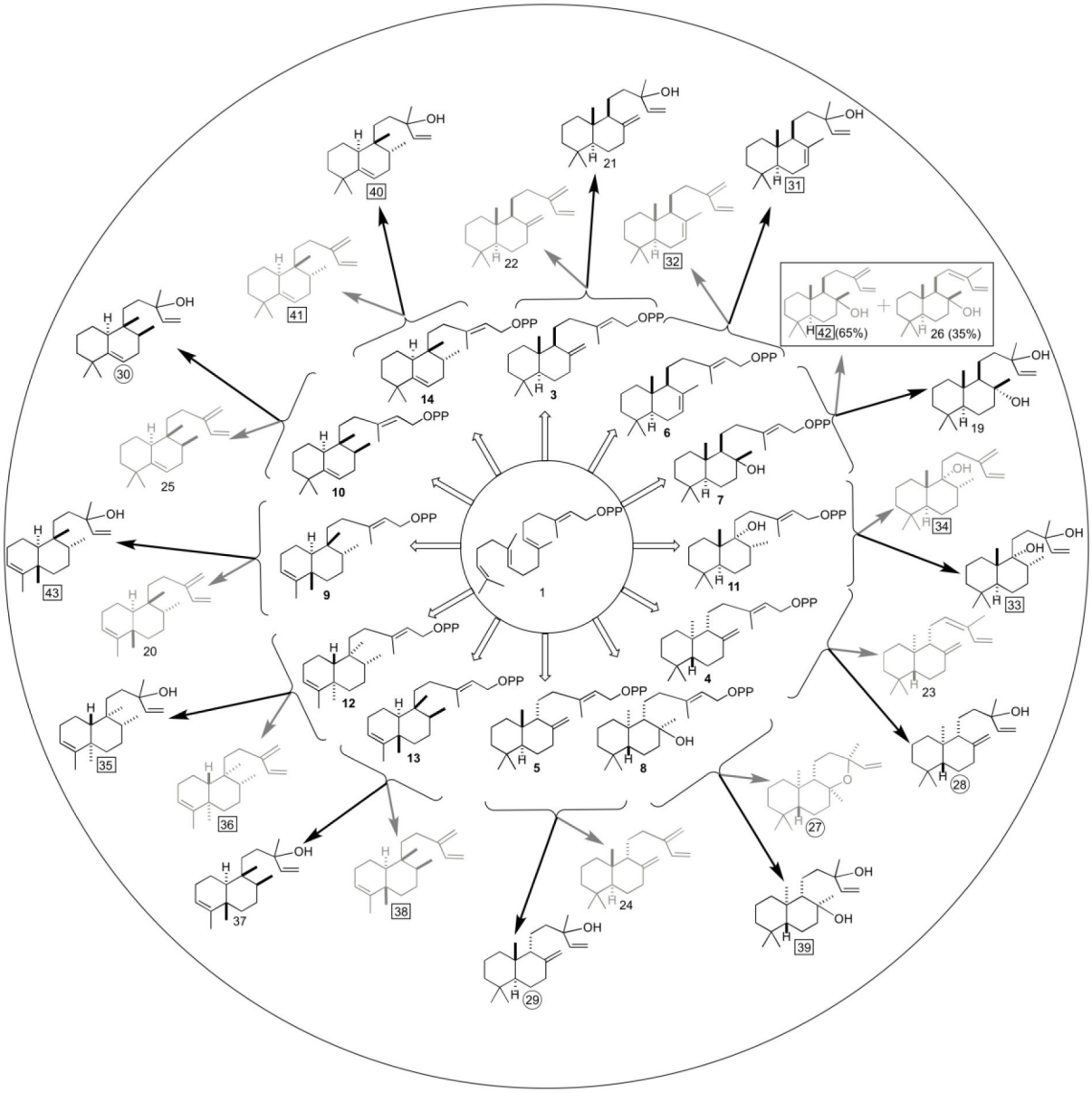

Fig. 6.

Summary of the combinatorial biosynthesis enabled by the extreme promiscuity of KgTS and SsSS. Show are the 12 bicyclic DTC products (**3–14**), derived from the general diterpene precursor GGPP (**1**), and the subsequent reactions catalyzed by KgTS (grey arrows and products) and SsSS (black arrows and products), with product ratio shown in the parenthesis when multiple products were observed (numbering as in the text, with the 12 unknown products boxed and the 5 for which only inefficient biosynthetic access was previously available circled).

Table 1

Class II diterpene cyclases (DTCs) used in this study.

No.[a]	DTC[b]	Origin	Product[c]	Reference
3	AgAS:D621A[d]	*Abies grandis*	Copalyl diphosphate (CPP)	(Peters et al., 2000)
4	ZmCPS2/An2	*Zea mays*	*ent*-CPP	(Harris et al., 2005)
5	OsCPS4	*Oryza sativa*	*syn*-CPP	(Xu et al., 2004)
6	SmCPS/KSL1: D500A/D504A[d]	*Selaginella moellendorffii*	*endo*-CPP	(Mafu et al., 2011)
7	NgCLS	*Nicotiana glutinosa*	8α-hydroxy-CPP	(Criswell et al., 2012)
8	AtCPS:H263A[e]	*Arabidopsis thaliana*	8β-hydroxy-*ent*-CPP	(Potter et al., 2014)
9	KgTPS	*Kitasatospora griseola*	terpentedienyl diphosphate	(Hamano et al., 2002)
10	MtHPS	*Mycobacterium tuberculosis*	tuberculosinyl diphosphate	(Mann et al., 2009a)
11	MvCPS1	*Marrubium vulgare*	peregrinol diphosphate	(Zerbe et al., 2014)
12	AtCPS:H263Y[f]	*Arabidopsis thaliana*	*ent*-kolavenyl diphosphate	(Potter et al., 2016b)
13	Haur_2145	*Herpetosiphon aurantiacus*	kolavenyl diphosphate	(Nakano et al., 2015)
14	OsCPS4:H501D[f]	*Oryza sativa*	*syn*-halimadienyl diphosphate	(Potter et al., 2016a)

[a] Compound numbering used here.

[b] Full names of these DTCs can be found in the abbreviation list.

[c] Previously assigned common names.

[d] Mutation(s) that blocks class I DTS activity of this bifunctional DTC/DTS.

[e] Mutant with hydrolyase activity.

[f] Mutant that yields rearranged product.

Table 2

Overview of diterpene products from this study.

No.[a]	Semi-systematic[b]	Common name[c]	DTS + S[d]	Identification[e]
15	–	β-springene	KgTS + **1**	Previous (Hamano et al., 2002)
16	–	(*Z*)-α-springene	KgTS + **1**	Previous (Hamano et al., 2002)
17	–	(*E*)-α-springene	KgTS + **1**	Previous (Hamano et al., 2002)
18	–	geranyllinool	SsSS + **1**	Comparison (Herde et al., 2008)
19	(8*R*,9*R*,10*S*,13*R*)-labda-14-en-8,13-diol	sclareol	SsSS + **7**	Previous (Ignea et al., 2015)
20	(5*S*,8*R*,9*R*,10*S*)-cleroda-3,13(16),14-triene	terpentetriene	KgTS + **9**	Previous (Nakano et al., 2010)
21	(9*S*,10*S*,13*R*)-labda-8(17),14-dien-13-ol	manool	SsSS + **3**	Previous (Ignea et al., 2015)
22	(9*S*,10*S*)-labda-8(17),13(16),14-triene	sclarene	KgTS + **3**	Previous (Nakano et al., 2010)
23	(9*R*,10*R*)-labda-8(17),12*Z*,14-triene	(*Z*)-biformene	KgTS + **4**	Previous (Nakano et al., 2010)
24	(9*R*,10*S*)-labda-8(17),13(16),14-triene	griseolaene	KgTS + **5**	Previous (Nakano et al., 2010)
25	(8*S*,9*R*,10*S*)-halimada-5,13(16),14-triene	tuberculosene	KgTS + **10**	Previous (Nakano et al., 2010)
26	(8*R*,9*R*,10*S*)-labda-12*Z*,14-dien-8-ol	*cis*-abienol	KgTS + **7** (35%)	Comparison (Zerbe et al., 2012)
27	(8*S*,9*S*,10*R*,13*S*)-labda-8,13-epoxy-14-ene	*ent*-manoyl oxide	KgTS + **8**	Comparison (Mafu et al., 2015)
28	(9*R*,10*R*,13*S*)-labda-8(17),14-dien-13-ol	*ent*-manool	SsSS + **4**	Comparison (Nakano et al., 2010)
29	(9*R*,10*S*,13*S*)-labda-8(17)14-dien-13-ol	vitexifolin A	SsSS + **5**	Comparison (Hoshino et al., 2011)
30	(8*S*,9*R*,10*S*,13*S*)-halimada-5,14-dien-13-ol	isotuberculosinol/nosyberkol	SsSS + **10**	Comparison (Hoshino et al., 2011)
31	(9*R*,10*S*)-labda-7,14-dien-13-ol	–	SsSS + **6**	This study (NMR)
32	(9*R*,10*S*)-labda-7,13(16),14-triene	–	KgTS + **6**	This study (NMR)
33	(8*R*,9*R*,10*S*)-labda-14-en-9,13-diol	viteagnusin D	SsSS + **11**	This study (NMR)
34	(8*R*,9*R*,10*S*)-labda-13(16),14-dien-9-ol	–	KgTS + **11**	This study (NMR)
35	(5*R*,8*R*,9*S*,10*R*)-cleroda-3,14-dien-13-ol	*ent*-kolavelool	SsSS + **12**	This study (NMR)
36	(5*R*,8*R*,9*S*,10*R*)-cleroda-3,13(16),14-triene	–	KgTS + **12**	This study (NMR)
37	(5*S*,8*S*,9*R*,10*S*)-cleroda-3,14-dien-13-ol	kolavelool	SsSS + **13**	This study (comparison to enantiomer, **35**)
38	(5*S*,8*S*,9*R*,10*S*)-cleroda-3,13(16),14-triene	–	KgTS + **13**	This study (comparison to enantiomer, **36**)
39	(8*S*,9*S*,10*R*,13*S*)-labda-14-en-8,13-diol	*ent*-sclareol	SsSS + **8**	This study (comparison to enantiomer, **19**)
40	(8*R*,9*R*,10*S*)-halimada-5,14-dien-13-ol	–	SsSS + **14**	This study (NMR)
41	(8*R*,9*R*,10*S*)-halimada-5,13(16),14-triene	–	KgTS + **14**	This study (NMR)
42	(8*R*,9*R*,10*S*)-labda-13(16),14-dien-8-ol	*iso*-abienol	KgTS + **7** (65%)	This study (NMR)
43	(5*S*,8*R*,9*R*,10*S*)-cleroda-3,14-dien-13-ol	–	SsSS + **9**	This study (NMR)

[a] Numbering used here.

[b] Only applicable to the labdane-related diterpenoids (i.e., not applicable to **15** – **18**, which are directly derived from **1**). Note that the absolute configurations are only listed for assignable chiral centers.

[c] Common names are those previously reported ("–" indicates that no name is available).

[d] Substrate (DTC product), numbered as defined in Table 1.

[e]Products were identified based on either ‘previous’ reports for these enzymes or GC-MS based ‘comparison’ to other previously reported DTS products (with accompanying reference), or were determined in ‘this study’ by NMR based structural analysis (or comparison to the characterized enantiomer).